HHS Public Access

Author manuscript

Exp Neurol. Author manuscript; available in PMC 2017 July 01.

Published in final edited form as:

Exp Neurol. 2016 July ; 281: 93–98. doi:10.1016/j.expneurol.2016.04.018.

AMYLOID-βPLAQUES DISRUPT AXON INITIAL SEGMENTS

Miguel A. Marin[1], **Jokubus Ziburkus**[2], **Joanna Jankowsky**[1], and **Matthew N. Rasband**[1,*]

[1]Department of Neuroscience, Baylor College of Medicine, One Baylor Plaza, Houston, TX 77030, USA

[2]Department of Biology and Biochemistry, University of Houston, Houston, TX 77204, USA.

Abstract

Amyloid-β (Aβ) plaques are one of the central pathologies of Alzheimer's disease (AD). Plaque formation in animal models of AD coincides with the appearance of synaptic abnormalities, aberrant neuronal excitability, and cognitive decline. Aβ plaques may disrupt neuronal excitability since they have been proposed to be synaptotoxic, to induce axonal varicosities and neurite breakage, and to significantly decrease spine density. Axon initial segments (AIS) also regulate neuronal excitability and help maintain neuronal polarity. Despite these essential functions, the effects of plaques on AIS structure have not been fully determined. Using a mouse AD model, we measured a significant decrease in the density of AIS up to 75 μm away from the center of fibrillar, thioflavin-labeled plaques. The reduction was observed in animals with both moderate and severe plaque loads, and was associated with increased densities of microglia near the plaques. Furthermore, animals with severe plaque loads had significantly reduced AIS lengths adjacent to Aβ plaques. These results suggest the local environment surrounding Aβ plaques may be harmful to the AIS. We propose that AIS loss is a previously unappreciated consequence of AD that could significantly impact brain function.

INTRODUCTION

Neurons have distinct electrically excitable domains including the axon initial segment (AIS), nodes of Ranvier, and synapses. The AIS integrates all somatodendritic synaptic input and initiates axonal action potentials (Kole et al., 2008; Kole and Stuart, 2012). The AIS also maintains neuronal polarity by segregating axonal and somatodendritic compartments (Hedstrom et al., 2008; Sobotzik et al., 2009), and excluding dendritic cargoes from the axon (Petersen et al., 2014). The AIS consists of a dense collection of cytoskeletal adaptor proteins, cell adhesion molecules, and voltage-gated ion channels (Rasband, 2010). Disruption of the AIS has dramatic impacts on brain function. For example, mice lacking the scaffolding protein ankyrinG (ankG) have no AIS and die at birth (Ho et al., 2014).

*Correspondence should be addressed to: Dr. Matthew Rasband, Department of Neuroscience, Baylor College of Medicine, One Baylor Plaza, Houston, TX 77030, ; Email: rasband@bcm.edu

Conflict of Interest: The authors declare no competing financial interests

Mutations in AIS-related genes are associated with neurological diseases, and models of stroke, traumatic injury, or other developmental and cognitive disorders all include disruption of the AIS as a common pathology (Buffington and Rasband, 2011; Kaphzan et al., 2011; Normand and Rasband, 2015; Schafer et al., 2009; Wimmer et al., 2010).

Alzheimer's disease (AD) is a chronic, progressive neurodegenerative disorder that is characterized by the deposition of amyloid-β (Aβ) peptide into plaques. Studies in animal models of AD suggest the microenvironment surrounding these plaques is synapto-toxic. For example, synapse loss, axonal varicosities, altered neural network integration, and neuronal hyperactivity in areas within or around Aβ plaques have been reported (Adalbert et al., 2009; Busche et al., 2008; Dong et al., 2007; Rudinskiy et al., 2012; Tsai et al., 2004). Previously, one study examined the effect of Aβ plaques on the AIS and reported a significant decrease in the number of GABAergic synapses innervating the AIS of cortical neurons near plaques, but no structural alterations to the AIS itself were observed (Leon-Espinosa et al., 2012). However, different levels of plaque burden were not examined, and a detailed analysis of AIS structure as a function of proximity to the plaque was not performed.

To determine if Aβ plaques affect AIS structure, we used a mouse model of AD that expresses a chimeric mouse amyloid precursor protein (APP) with a humanized Aβ domain and Swedish (KM670/671NL) and Indiana (V617F) mutations under a tetO promoter. When crossed to CaMKIIα-TTA (tetracycline transactivator) mice (hereafter referred to as APP/TTA mice), offspring overexpress the APP transgene in forebrain neurons. Compared to non-transgenic mice, APP/TTA mice express 5-10 times more APP protein and display early onset amyloid pathology. Aβ pathology increases with time such that by 6 months of age, APP/TTA mice display moderate pathology with Aβ plaques apparent throughout the cortex and hippocampus; by 11 months of age, APP/TTA mice have severe plaque burden with Aβ plaques throughout the cortex, hippocampus, thalamus, and striatum (Figs. 1A, B) (Jankowsky et al., 2005). Using these mice, we find that Aβ plaques cause a significant decrease in both number and length of AIS, a significant increase in microglia, and that AIS alterations depend on both proximity to the plaque and plaque load. Our results suggest that altered AIS structure may contribute to the pathophysiology of AD.

MATERIALS AND METHODS

Animals

The APP/TTA mice were previously described (Jankowsky et al., 2005). Bigenic mice of both sexes were used for analysis. Single transgenic CaMKIIα-TTA (TTA) and non-transgenic (NTG) littermates were used as controls. All experiments were performed in compliance with the National Institutes of Health Guide for the Care and Use of Laboratory Animals and were approved by the Baylor College of Medicine Institutional Animal Care and Use Committee. A minimum of 3 animals per genotype was used at each time point.

Immunostaining

Mice were killed by isoflurane overdose followed by cervical dislocation. Upon decapitation, brains were quickly removed and fixed in ice cold 4% PFA (pH 7.2, 1hr)

followed by 30% sucrose (0.1M phosphate buffer (PB)) immersion for 2 days. Fixed brains were then frozen in OCT medium and sectioned into 35μm thick coronal sections. Sections were then stored in antifreeze buffer (glycerol, ethylene glycol, 0.1M PB) until used for immunostaining. For immunostaining, sections were washed in 0.1M PB and blocked in 0.1M PB with 0.3% Triton X-100 detergent and 5% goat serum. Sections were incubated in primary antibodies overnight. The following antibodies were used: rabbit polyclonal anti-βIV spectrin (Yang et al., 2004), mouse monoclonal anti-NeuN (Millipore), mouse monoclonal anti-GFAP (neuromab, clone N206A/8), and rabbit polyclonal anti-Iba1 (Abcam). Primary antibodies were then labeled using AlexaFluor-conjugated secondary antibodies (Invitrogen). To detect nuclei, sections were counterstained with Hoechst 33258 pentahydrate (Invitrogen). Amyloid plaques were detected by counterstaining with thioflavin-S (Sigma) or by amyloid plaque autofluorescence. Sections were visualized with a Zeiss Imager.Z1 fluorescent microscope with an Apotome attachment.

Image analysis

40x z-stacks were captured in the superficial layer of the cortex (approximately layers 2-4) in three regions of the mouse cortex: M1, S1, or V1. Images were captured using structured illumination (Zeiss). In AD brains, three concentric circles (regions of interest, ROI) of 50, 100, and 150 μm diameter were placed over individual plaques of equivalent dimensions (Figs. 1D and E). AIS number and length, and the number of nuclei or microglia were counted within each annulus and within the inner circle. Similar measurements were made in corresponding regions of cortex from TTA and NTG mice. All measurements were performed using ImageJ (NIH). AIS were defined as βIV spectrin-labeled segments greater than 10 μm in length. For all quantifications we imaged 3 plaques (or equivalent control regions) per mouse, with 3 mice of each genotype at each age; we pooled data from the three regions of the cortex. If an AIS crossed two ROIs it was included in the outermost ROI. Measurements were compared in Prism using two-way ANOVA with the Bonferroni multiple comparisons post test.

RESULTS

AIS are essential for action potential initiation and the maintenance of neuronal polarity. AIS consist of a high density of voltage-gated ion channels, cell adhesion molecules, and scaffolding proteins including ankG and βIV spectrin. We previously showed that ankG and βIV spectrin are potent targets for calpain-mediated proteolysis in diverse CNS injuries (Schafer et al., 2009). To determine if Aβ plaques disrupt the AIS, we immunostained brain sections of APP/TTA mice using antibodies against βIV spectrin and NeuN (Fig. 1C). We found that Aβ plaques displaced neurons and AIS such that AIS frequently bend or take circuitous trajectories around, but seldom through, Aβ plaques. We frequently observed Hoechst-labeled nuclei (not associated with NeuN or βIV spectrin immunoreactivity) surrounding and within plaques (Fig. 1C). We identified and observed plaques in two wasy: Thioflavin-S labeling or plaque autofluorescence (Fig. 2A). In animals with moderate (~6 months) and severe (~11 months) plaque burden, we occasionally found AIS that traversed, or were at the edges of plaques (Figs. 2B-D, arrows). These AIS were fragmented, shorter, and thinner than those further away from the plaque.

To determine if axons traverse Aβ plaques, we immunostained axons using antibodies against neurofilament-M (NF-M). Whereas control brains had strongly labeled axons that were often oriented in parallel trajectories (Fig. 2E), brains with a heavy plaque burden (11 months) had axons with random orientations and many dystrophic, degenerating axons including axonal torpedoes, large NF-M labeled swellings, and transections at the site of contact with the plaque (Figs. 2F and G, arrows). These results suggest that plaques are harmful to axons and either directly or indirectly cause their degeneration.

To determine if different levels of Aβ plaque burden and proximity to a plaque affect the density of cells in the cortex, we quantified the total number of Hoechst-labeled cells as a function of distance from the center of a plaque (Fig. 1D; regions A, B, and C), and compared these values to the density of cells found in control TTA and NTG mice. At 6 (Fig. 3A) and 11 months of age (Fig. 3B) Aβ plaques were readily identified in the cortex of APP/TTA mice by thioflavin-S staining. We found that at both 6 and 11 months of age there was no significant difference in the total number of cells within each area analyzed between mutant and control mice (Fig. 3C).

How can there be an equivalent number of cells when plaques clearly displace axons and even neurons (Figs. 1C, 2F, and 4A)? We reasoned that the deposition of Aβ may result in the proliferation or recruitment of glial and inflammatory cells. To test this possibility, we immunostained 11 month old APP/TTA mice using antibodies against GFAP or Iba-1 to label astrocytes or microglia, respectively (Figs. 4B and 4C). Although we found hypertrophic astrocytes in the vicinity of the plaque, we did not find any increase in the density of these cells. In contrast, we observed a shell of activated microglia encapsulating the Aβ plaque. Compared to control brains (Fig. 4D), we also measured a significant increase in the density of microglia surrounding plaques (Fig. 4E). Thus, the apparent preservation of cell number in each region reflects the recruitment and/or proliferation of microglia near the plaque.

What is the consequence of Aβ production and deposition in plaques on AIS number and length, and how does increasing plaque load affect these properties? To answer these questions we counted AIS number and length in each region of interest (ROI; Fig. 1E). At 6 months of age (Fig. 5A) we found Aβ plaques that were readily identified by autofluorescence. We measured a significant decrease in the number of AIS in all ROIs from APP/TTA mice compared to NTG controls (Fig. 5B). Despite the decrease in the density of AIS, in 6 month-old mice we did not detect any difference in the average length of AIS between APP/TTA and control mice (Fig. 5C). At 11 months of age APP/TTA mice had even more severe plaque burden compared to 6 month old mice (Figs. 1A, B). Again, Aβ plaques were readily identified by autofluorescence and AIS were visualized by immunostaining for βIV spectrin (Fig. 5D). We found that in all APP/TTA ROIs there was a significant reduction in the number of AIS compared to both TTA and NTG controls (Fig. 5E). Indeed, AIS were only rarely observed in the ROI containing the plaque itself, and the number of AIS in the next largest ROI had only half the number of AIS as control mice. When AIS were present in the APP/TTA plaque-containing ROIs, they were significantly shorter than those found in all other surrounding annuli or in control mice (Fig. 5F).

Together, these results support the conclusion that both Aβ burden and plaques themselves either directly, or indirectly, affect both the number and structure of AIS.

DISCUSSION

We used a mouse model of AD to investigate how Aβ plaque load and proximity affect the number and structure of AIS. AIS are essential for proper nervous system function since they act as the anatomical and physiological connection between neuronal input and output. Specifically, the AIS integrates synaptic input to initiate action potentials in axons and the AIS controls the polarized distribution of axonal and somatodendritic proteins (Rasband, 2010). Here, we showed two main results: 1) increasing plaque load decreases AIS density in the vicinity of a plaque, and 2) plaque proximity affects AIS length.

What mechanisms explain the reduction in AIS density? AIS reduction may result from neuronal displacement, neuron death, disruption of the AIS by Aβ, perhaps through calpain-mediated proteolysis of the AIS cytoskeleton, or a combination of these factors. Since many axon trajectories go around, rather than through plaques, we conclude that plaques cause the physical displacement of neurons and axons. Indeed, many axons that contact the plaque are transected or misshapen. However, a reduction in AIS density simply due to displacement of cells should increase AIS density in ROIs further from the plaque. This was not the case. Although the size of individual plaques did not increase significantly with plaque load (1603±270 μm^2 and 2161±24 μm^2, p=0.1, for 6 and 11 month old APP/TTA mice, respectively), AIS density progressively decreased with increasing plaque load, suggesting a specific effect of Aβ. Disruption of the spectrin-based axonal cytoskeleton may cause fragmentation of AIS (Galiano et al., 2012), as we observed in the APP/TTA mice (Figs. 2B, 2C). Thus, our measurement of AIS density may be an underestimate since we only counted AIS that were 10 μm or longer.

Although we did observe a significant increase in the number of microglia immediately surrounding plaques, indicating local inflammation, we did not see any change in the number of neurons, astrocytes, or microglia in ROIs farther away from the plaque. Nevertheless, the significant loss of AIS near Aβ plaques and the associated reduction in AIS length observed in this ROI may reflect a direct effect of activated microglia on the AIS, rather than an effect of Aβ on the AIS. On the other hand, Aβ has been shown to induce Ca^{2+} currents in neurons (Busche et al., 2008) and has been proposed to be a major contributor to the pathogenesis of AD (Price et al., 1998; Small et al., 2009). Intriguingly, the main AIS scaffolding proteins ankyrinG and βIV spectrin are potent substrates for Ca^{2+} dependent calpain-mediated proteolysis, and their proteolysis results in loss of AIS ion channel clustering (Schafer et al., 2009). Some AD patients have autoantibodies against ankG, and the presence of these antibodies is correlated with slower rates of cognitive decline (Santuccione et al., 2013). Indeed, active immunization with ankG promoted the reduction of β-amyloid pathology in a mouse model of AD.

How would loss or remodeling of AIS influence nervous system function? The complete loss of the AIS in a neuron would be expected to result in protein mislocalization and failure to integrate synaptic inputs or to properly generate action potentials. Consistent with this

notion, previous studies have shown that the barrier functions of the AIS are disrupted in AD. Specifically, the distribution of tau is regulated by the AIS, and it is missorted into somatodendritic domains in AD (Li et al., 2011). Reductions in AIS length would be expected to reduce overall neuronal excitability, however this may be a homeostatic response to Aβ excitoxicity. Our results complement previous studies of the AIS where GABAergic innervation of the AIS was perturbed in mouse models of AD (Leon-Espinosa et al., 2012).

Together, these observations suggest that AIS loss or remodeling may be an important component of the cognitive impairment and circuit dysfunction observed in AD.

Acknowledgements

This work was supported by grants from the US National Institutes of Health (NS069688 and NS044916 to M.N.R. and DP2 OD001734-02S1 to J.J.).

REFERENCES

Adalbert R, Nogradi A, Babetto E, Janeckova L, Walker SA, Kerschensteiner M, Misgeld T, Coleman MP. Severely dystrophic axons at amyloid plaques remain continuous and connected to viable cell bodies. Brain. 2009; 132:402–416. [PubMed: 19059977]

Buffington SA, Rasband MN. The axon initial segment in nervous system disease and injury. Eur J Neurosci. 2011; 34:1609–1619. [PubMed: 22103418]

Busche MA, Eichhoff G, Adelsberger H, Abramowski D, Wiederhold KH, Haass C, Staufenbiel M, Konnerth A, Garaschuk O. Clusters of hyperactive neurons near amyloid plaques in a mouse model of Alzheimer's disease. Science. 2008; 321:1686–1689. [PubMed: 18802001]

Dong H, Martin MV, Chambers S, Csernansky JG. Spatial relationship between synapse loss and beta-amyloid deposition in Tg2576 mice. J Comp Neurol. 2007; 500:311–321. [PubMed: 17111375]

Galiano MR, Jha S, Ho TS, Zhang C, Ogawa Y, Chang KJ, Stankewich MC, Mohler PJ, Rasband MN. A distal axonal cytoskeleton forms an intra-axonal boundary that controls axon initial segment assembly. Cell. 2012; 149:1125–1139. [PubMed: 22632975]

Hedstrom KL, Ogawa Y, Rasband MN. AnkyrinG is required for maintenance of the axon initial segment and neuronal polarity. J Cell Biol. 2008; 183:635–640. [PubMed: 19001126]

Ho TS, Zollinger DR, Chang KJ, Xu M, Cooper EC, Stankewich MC, Bennett V, Rasband MN. A hierarchy of ankyrin-spectrin complexes clusters sodium channels at nodes of Ranvier. Nat Neurosci. 2014; 17:1664–1672. [PubMed: 25362473]

Jankowsky JL, Slunt HH, Gonzales V, Savonenko AV, Wen JC, Jenkins NA, Copeland NG, Younkin LH, Lester HA, Younkin SG, Borchelt DR. Persistent amyloidosis following suppression of Abeta production in a transgenic model of Alzheimer disease. PLoS medicine. 2005; 2:e355. [PubMed: 16279840]

Kaphzan H, Buffington SA, Jung JI, Rasband MN, Klann E. Alterations in intrinsic membrane properties and the axon initial segment in a mouse model of angelman syndrome. J Neurosci. 2011; 31:17637–17648. [PubMed: 22131424]

Kole MH, Ilschner SU, Kampa BM, Williams SR, Ruben PC, Stuart GJ. Action potential generation requires a high sodium channel density in the axon initial segment. Nat Neurosci. 2008; 11:178–186. [PubMed: 18204443]

Kole MH, Stuart GJ. Signal processing in the axon initial segment. Neuron. 2012; 73:235–247. [PubMed: 22284179]

Leon-Espinosa G, DeFelipe J, Munoz A. Effects of amyloid-beta plaque proximity on the axon initial segment of pyramidal cells. Journal of Alzheimer's disease: JAD. 2012; 29:841–852. [PubMed: 22337828]

Li X, Kumar Y, Zempel H, Mandelkow EM, Biernat J, Mandelkow E. Novel diffusion barrier for axonal retention of Tau in neurons and its failure in neurodegeneration. EMBO J. 2011; 30:4825–4837. [PubMed: 22009197]

Normand EA, Rasband MN. Subcellular patterning: axonal domains with specialized structure and function. Dev Cell. 2015; 32:459–468. [PubMed: 25710532]

Petersen JD, Kaech S, Banker G. Selective microtubule-based transport of dendritic membrane proteins arises in concert with axon specification. J Neurosci. 2014; 34:4135–4147. [PubMed: 24647935]

Price SA, Held B, Pearson HA. Amyloid beta protein increases Ca2+ currents in rat cerebellar granule neurones. Neuroreport. 1998; 9:539–545. [PubMed: 9512403]

Rasband MN. The axon initial segment and the maintenance of neuronal polarity. Nat Rev Neurosci. 2010; 11:552–562. [PubMed: 20631711]

Rudinskiy N, Hawkes JM, Betensky RA, Eguchi M, Yamaguchi S, Spires-Jones TL, Hyman BT. Orchestrated experience-driven Arc responses are disrupted in a mouse model of Alzheimer's disease. Nat Neurosci. 2012; 15:1422–1429. [PubMed: 22922786]

Santuccione AC, Merlini M, Shetty A, Tackenberg C, Bali J, Ferretti MT, McAfoose J, Kulic L, Bernreuther C, Welt T, Grimm J, Glatzel M, Rajendran L, Hock C, Nitsch RM. Active vaccination with ankyrin G reduces β-amyloid pathology in APP transgenic mice. Mol Psych. 2013; 18:358–368.

Schafer DP, Jha S, Liu F, Akella T, McCullough LD, Rasband MN. Disruption of the axon initial segment cytoskeleton is a new mechanism for neuronal injury. J Neurosci. 2009; 29:13242–13254. [PubMed: 19846712]

Small DH, Gasperini R, Vincent AJ, Hung AC, Foa L. The role of Abeta-induced calcium dysregulation in the pathogenesis of Alzheimer's disease. Journal of Alzheimer's disease: JAD. 2009; 16:225–233. [PubMed: 19221414]

Sobotzik JM, Sie JM, Politi C, Del Turco D, Bennett V, Deller T, Schultz C. AnkyrinG is required to maintain axo-dendritic polarity in vivo. Proc Natl Acad Sci U S A. 2009; 106:17564–17569. [PubMed: 19805144]

Tsai J, Grutzendler J, Duff K, Gan WB. Fibrillar amyloid deposition leads to local synaptic abnormalities and breakage of neuronal branches. Nat Neurosci. 2004; 7:1181–1183. [PubMed: 15475950]

Wimmer VC, Reid CA, So EY, Berkovic SF, Petrou S. Axon initial segment dysfunction in epilepsy. J Physiol. 2010; 588:1829–1840. [PubMed: 20375142]

Yang Y, Lacas-Gervais S, Morest DK, Solimena M, Rasband MN. BetaIV spectrins are essential for membrane stability and the molecular organization of nodes of Ranvier. J Neurosci. 2004; 24:7230–7240. [PubMed: 15317849]

SIGNIFICANCE STATEMENT

This paper demonstrates that neurons near Aβ plaques have disrupted axon initial segments. Loss or disruption of AIS is predicted to have detrimental consequences for brain function.

Highlights

- Neurons near Aβ plaques have disrupted axon initial segments
- Neurons near Aβ plaques have shorter axon initial segments
- Disruption of AIS is correlated with Aβ plaque load
- Disruption of AIS is correlated with increased densities of microglia

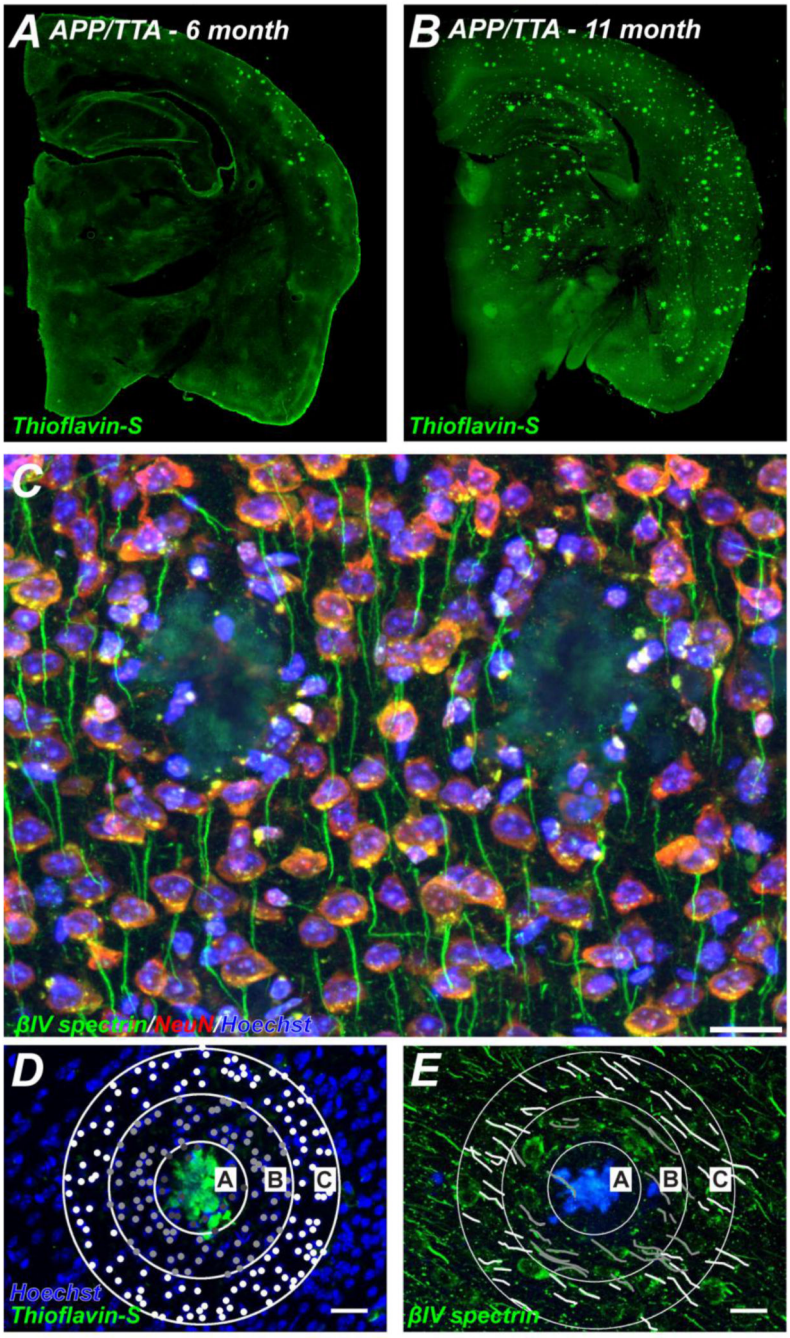

Figure 1.

Plaque burden and pathology of APP/TTA mice. A, B, Coronal sections of 6 (B) and 11 month old (B) APP/TTA mice labeled using thioflavin-S to visualize Aβ plaques. C, Cortex from 11 month old APP/TTA mouse labeled using antibodies against βIV spectrin (green) to visualize AIS, NeuN (red) to label neuronal cell bodies, and Hoechst (blue) to detect nuclei. Scale bar = 20 μm. D, E, For quantification of the number of cells (D) and the number of AIS (E), three concentric rings with diameters of 50, 100, and 150 μm were centered on a plaque and used to define three regions of interest (ROIs A, B, and C). When nuclei were

labeled with Hoechst (blue; D), plaques were detected using thioflavin-S (green; D). When AIS were detected using antibodies against βIV spectrin (green; E), plaques were visualized by their autofluorescence (blue; E). Scale bar = 20 μm.

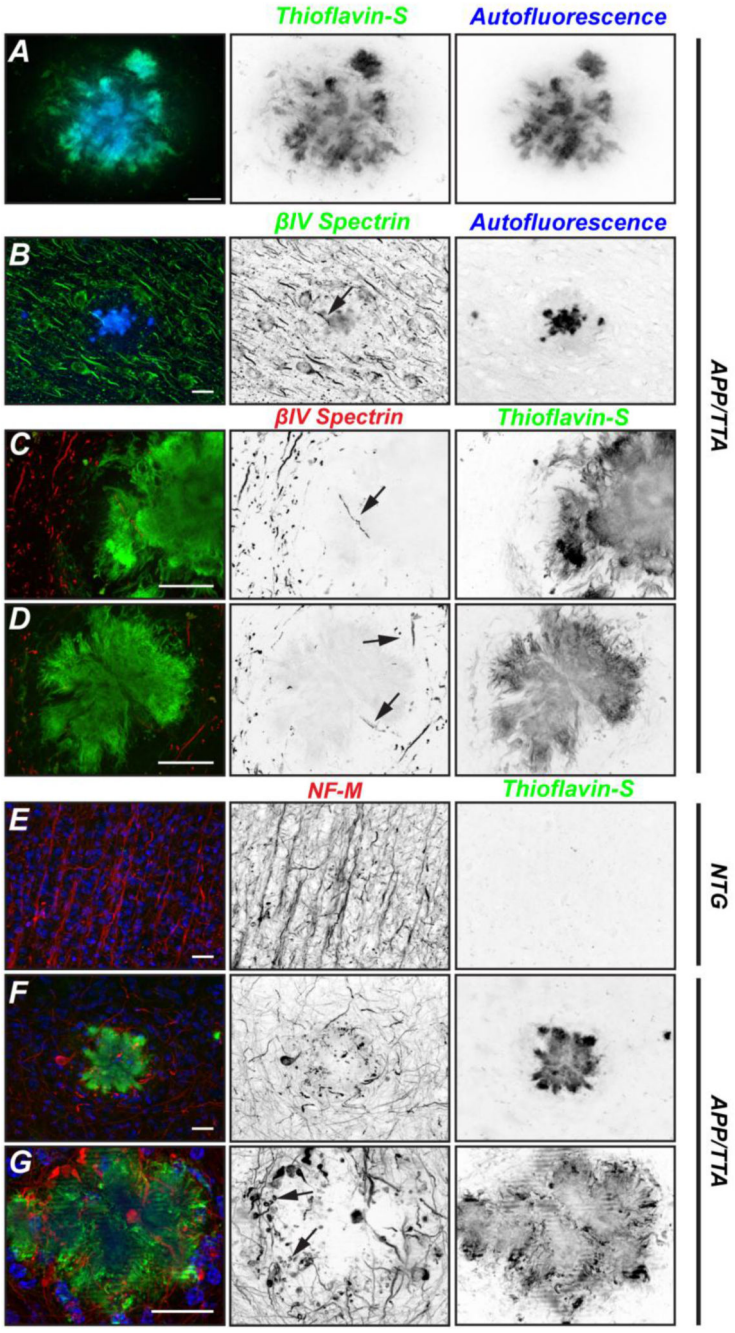

Figure 2.

Axons are disrupted by Aβ plaques. A, Detail of Aβ plaque shown by Thioflavin-S labeling (green) and autofluorescence (blue). B, Brain section from 6 month old APP/TTA mouse immunolabeled for βIV spectrin (green). The plaque can be visualized by autofluorescence (blue). C, D, 11 month old brain sections from APP/TTA mice labeled for βIV spectrin (red) or Thioflavin-S to detect Aβ plaques. Arrows indicate AIS within or adjacent to plaques. E-G, Immunostaining of 11 month old non-transgenic (NTG; E) or APP/TTA brains labeled for neurofilament-M (NF-M; red), thioflavin-S (green), or Hoechst (blue). In G, arrows

indicate transected and degenerating axons. NB: the lines in Fig. 2G result from the long exposure times required for the optical sectioning performed with the apotome attachment during imaging. Scale bars = 20 μm.

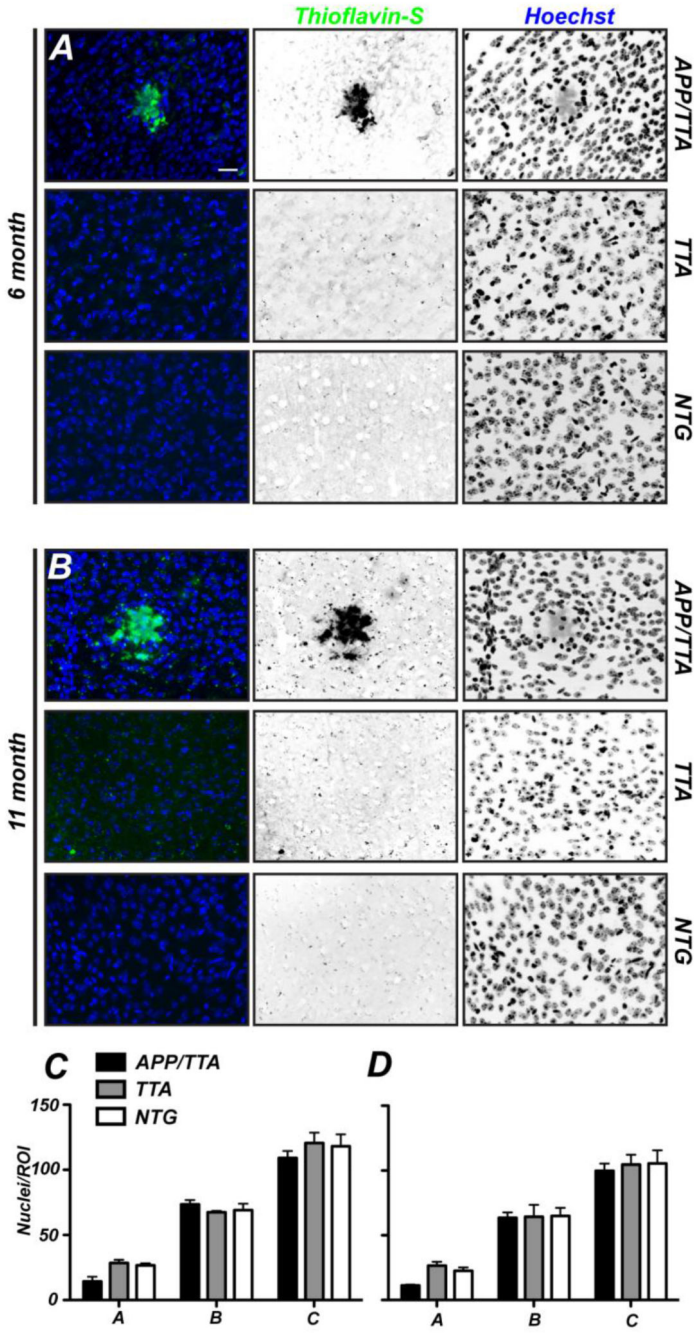

Figure 3.

Neither plaques nor plaque load alter the density of cells. A, B, Nuclei in cortices of 6 and 11 month old APP/TTA, TTA, and non transgenic (NTG) mice were labeled using Hoechst (blue). Aβ plaques were detected by thioflavin-S labeling. Scale bar = 20 μm. C, D, Quantification of the number of Hoechst-labeled nuclei in concentric ROIs in 6 (C) and 11 month old mice (D). All post hoc comparisons were not significant. N=3 mice per genotype.

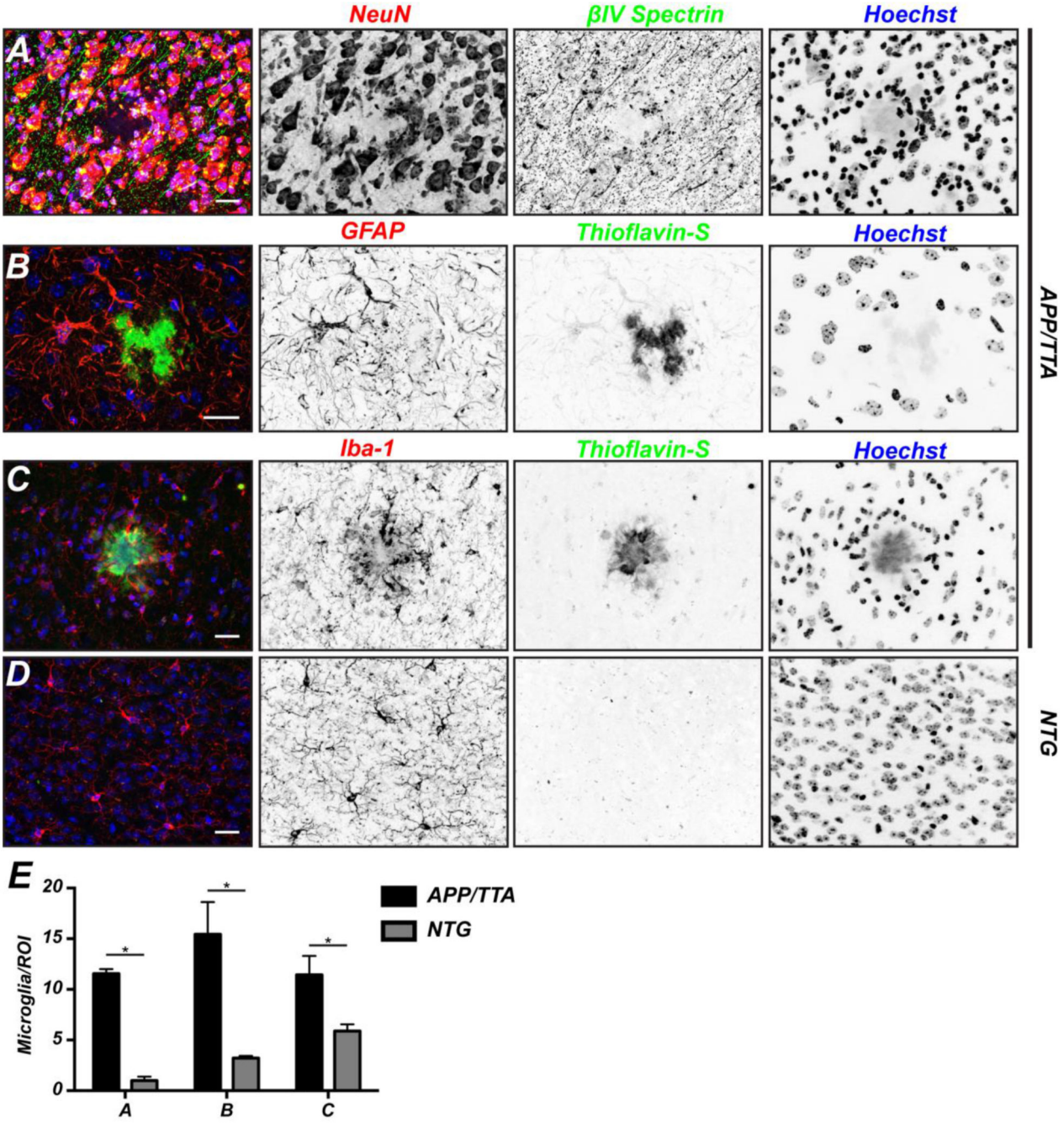

Figure 4.

Activated microglia surround Aβ plaques. A, To visualize neurons, coronal sections of 11 month old APP/TTA mice were labeled for βIV spectrin (green), NeuN (red), and Hoechst (blue). Scale bar = 20 μm. B, To visualize astrocytes, coronal sections of 11 month old APP/TTA mice were labeled for thioflavin-S (green), GFAP (red), and Hoechst (blue). Scale bar = 20 μm. C, To visualize microglia, coronal sections of 11 month old APP/TTA mice were labeled for thioflavin-S (green), Iba-1 (red), and Hoechst (blue). Scale bar = 20 μm. D,

Quantification of the number of microglia surrounding Aβ plaques. Analyses were performed on 11 month old NTG and APP/TTA mice. N=3 mice per genotype. *, $p<0.05$.

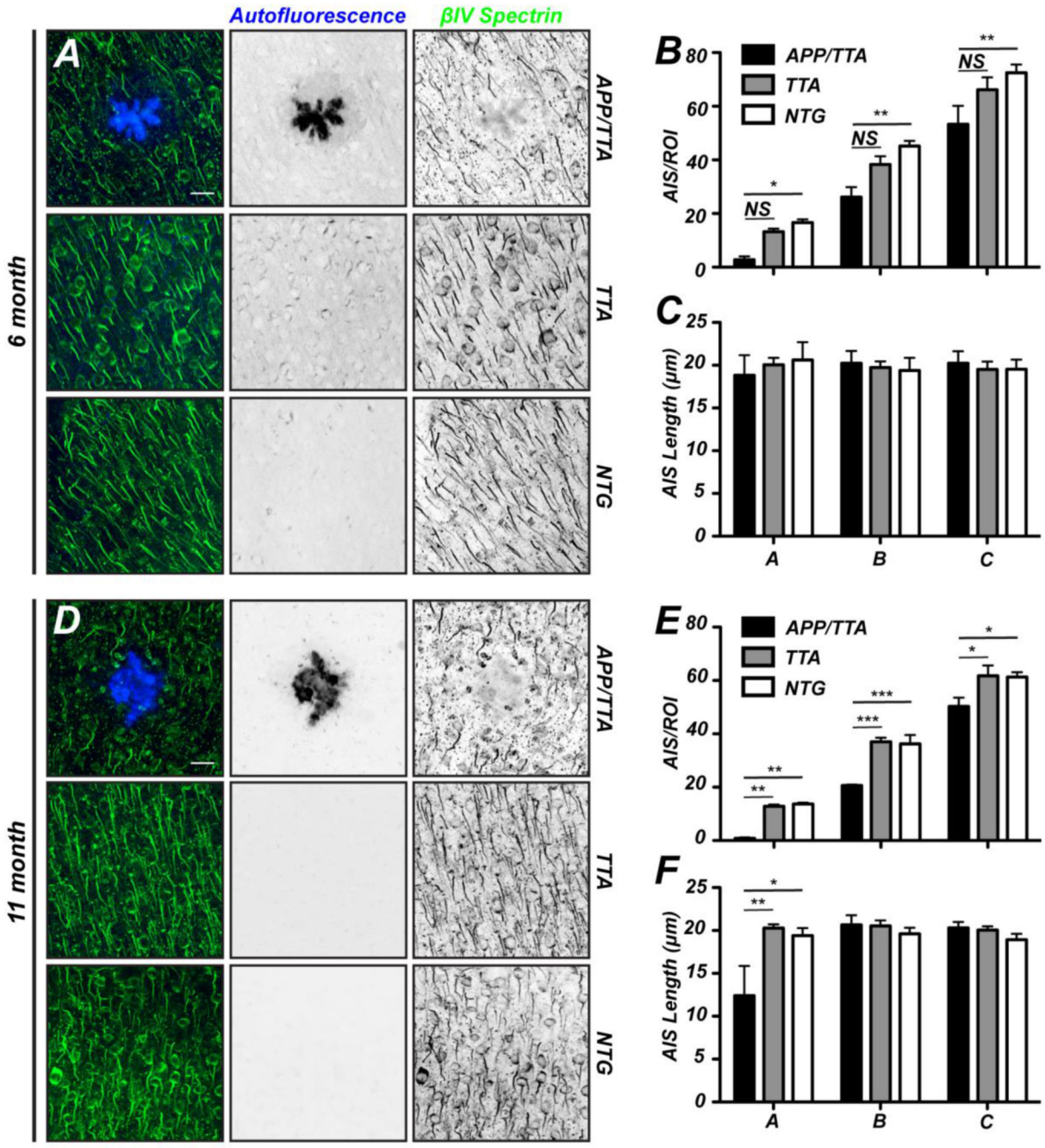

Figure 5.

Both plaque load and proximity disrupt AIS. A, D, Coronal sections of 6 (A) and 11 month old (D) APP/TTA, TTA, and NTG mice labeled using antibodies against βIV spectrin to visualize AIS and autofluorescence to visualize plaques. Scale bar = 20 μm. B, E, The number of AIS/ROI in 6 (B) and 11 (E) month old APP/TTA, TTA, and NTG mice. C, F, Average AIS length in 6 (C) and 11 (F) month old APP/TTA, TTA, and NTG mice. Post hoc

comparisons were not significant unless otherwise indicated; *, $p<0.05$; **, $p<0.001$. N=3 mice per genotype.